9

Examples of Application

In this chapter a number of applications of the PIV technique will be described, contributed by leading PIV experts from different research establishments and universities worldwide. A complete list of authors and their affiliation is given in the acknowledgement at the beginning of this book.

Primarily, the objective of presenting these applications is to show how the PIV technique has spread out to the most different research areas. However, it is of even higher importance to gain the reader access to a wide variety of ideas for PIV measurements by presenting many different applications in fundamental or industrial research. For each experiment the most important parameters of the object under investigation, of the illumination and recording setup, etc. will be given. These data together with the hints and tricks briefly described and the references to further, more detailed, literature may be useful for the reader when trying to solve problems of his own application.

9.1 Liquid Flows

9.1.1 Vortex-Free-Surface Interaction

Contributed by:
C. Willert, M. Gharib

The present example was chosen to illustrate the possibility of PIV in providing time-resolved measurements in low-speed flows, which is of importance in many fluid mechanical investigations. Time resolution is possible when the image frame rate exceeds the time scales present in the flow. For this investigation the frame rate of the utilized video equipment was 30 Hz (RS-170) resulting in an image-pair rate of 15 Hz using the frame–straddling approach, whereas the time-scales in the flow were longer than $1/10^{th}$ of a second. The PIV parameters used for this investigation are listed in table 9.1.

Table 9.1. PIV recording parameters for vortex–free-surface interaction.

Flow geometry	Nearly two-dimensional flow aligned with the light sheet
Maximum in-plane velocity	$U_{\max} \approx 10\,\mathrm{cm/s}$
Field of view	$103 \times 97\,\mathrm{mm}^2$
Interrogation volume	$6.4 \times 6.4 \times 1.5\,\mathrm{mm}^3$ ($H \times W \times D$)
Dynamic spatial range	DSR $\approx 16:1$
Dynamic velocity range	DVR $\approx 100:1$
Observation distance	$z_0 \approx 1.5\,\mathrm{m}$ (through glass/water)
Recording method	double frame/single exposure
Ambiguity removal	frame separation (frame-straddling)
Recording medium	frame transfer CCD (512×480 pixel)
Recording lens	$f = 50\,\mathrm{mm}$, $f_\# = 1.8$
Illumination	5 W CW argon-ion laser, mechanical shutter
Pulse delay	$\Delta t = 10\,\mathrm{ms}$
Pulse duration	2 ms
Seeding material	silver-coated, glass spheres ($d_\mathrm{p} \approx 10\,\mu\mathrm{m}$)

The vortex-pair flow under investigation is motivated in the context of understanding the fundamentals of the interaction of vortical structures with a free surface [306]. The vortex pair was generated by a pair of counter-rotating flaps whose sharp tips were located at $y \approx -10\,\mathrm{cm}$. Once the flaps were closed the separation vortex from each tip formed a symmetric vortex pair which propagated towards the surface within two seconds. The interesting interaction events typically took place in the following 2–5 seconds. This means that of the order of O[10 s] worth of PIV data were needed to resolve a single interaction process. This translated to 300 separate PIV recordings, which were acquired using a computer-based, real-time digitization and hard-disk array.

Figure 9.1 shows four selected instantaneous PIV velocity and corresponding vorticity fields from a 150 image-pair sequence. Since the flow was repeatable, it was imaged in several different planes in order to reconstruct the entire flow field. Using the circulation measurement schemes described in section 6.5.1 time-resolved circulation measurements of the vortex structures could be obtained from the velocity maps to study the vortex dynamics at the surface, namely, vortex reconnection and dissipation. Further details on this as well as related experiments can be found in Willert [305] and Weigand & Gharib [304].

9.1.2 Study of Thermal Convection and Couette Flows

Contributed by:

C. Böhm, C. Willert, H. Richard

These experimental investigations of flows by means of PIV have been carried out by DLR in cooperation with the Center of Applied Space Technology

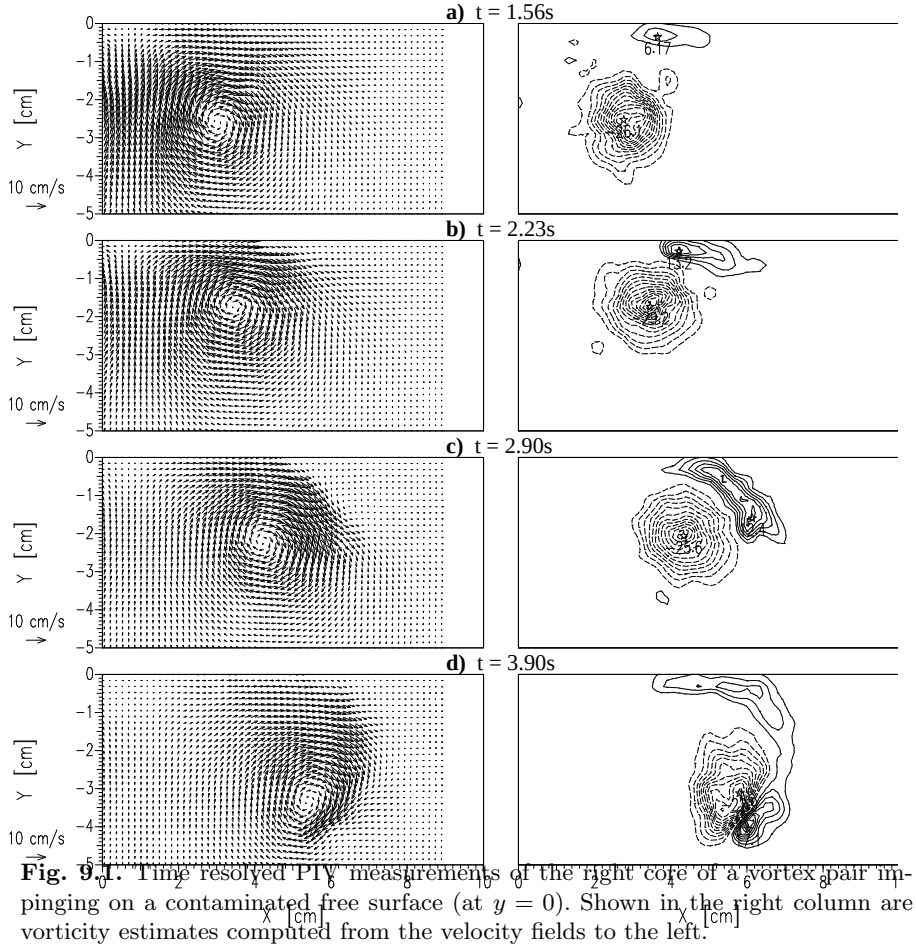

Fig. 9.1. Time resolved PIV measurements of the right core of a vortex pair impinging on a contaminated free surface (at $y = 0$). Shown in the right column are vorticity estimates computed from the velocity fields to the left.

and Microgravity (ZARM), University of Bremen, in order to complete their numerical simulations and LDV measurements [301]. The experimental setup is shown in figure 9.2. The PIV parameters used for this investigation are listed in table 9.2.

A fluid (silicone oils M20 and M3) seeded with 10 μm diameter glass particles with a volumetric mass near 1.05 g/cm^3 and a refraction index of $n = 1.55$, is filled in the gap between two concentric spheres. The outer sphere is composed of two transparent acrylic glass hemispheres (refraction index of $n = 1.491$), with a radius of 40.0 mm, and the inner sphere is made out of aluminum with a radius of 26.7 mm. To minimize optical distortions because of the curvature of the model, the outer sphere is included in a rectangular

Table 9.2. PIV recording parameters for thermal convection.

Flow geometry	$U_\infty = 0.5\,\mathrm{cm/s}$ parallel to light sheet
Maximum in-plane velocity	$U_{\max} \approx 0.5\,\mathrm{cm/s}$
Field of view	$50 \times 40\,\mathrm{mm}^2$
Interrogation volume	$1.6 \times 1.6 \times 2\,\mathrm{mm}^3$ $(H \times W \times D)$
Dynamic spatial range	DSR $\approx 24:1$
Dynamic velocity range	DVR $\approx 200:1$
Observation distance	$z_0 \approx 1.5\,\mathrm{m}$
Recording method	dual frame/single exposure
Ambiguity removal	frame separation
Recording medium	full frame interline transfer CCD $(782 \times 582\,\mathrm{pixel})$
Recording lens	$f = 100\,\mathrm{mm}$ $f_\# = 2.8$ to 22
Illumination	continuous argon-Ion laser, 1 watt, internal shutter of camera
Pulse delay	$\Delta t = 40\,\mathrm{ms}$
Seeding material	glass particles ($d_\mathrm{p} \approx 10\,\mu\mathrm{m}$)

cavity filled with silicone oil to provide a plane liquid–air interface and reduce optical refraction.

To study the thermal convection flows, the inner sphere is heated homogeneously up to 45°C whereas the outer sphere is held at constant temperature. Six temperature sensors are installed on both spheres as indicated in figure 9.2. A 25 Hz CCD camera with an internal shutter (40 ms between each frame) was used in combination with a continuous argon-ion laser. This was possible because of the low velocity flow studied ($\approx 0.5\,\mathrm{cm/s}$). A 100 mm Zeiss Makro Planar objective lens was used during the flow measurements with a $f_\#$ number of 2.8. For a magnification between 1/2 and 1/4, and a f-number of $f_\# = 11$, the particle image diameters are in the range between 22 and 18 μm,

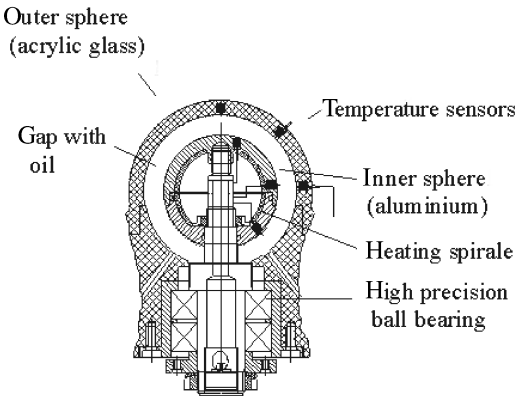

Fig. 9.2. The experimental apparatus to study the thermal convection and the Taylor flow.

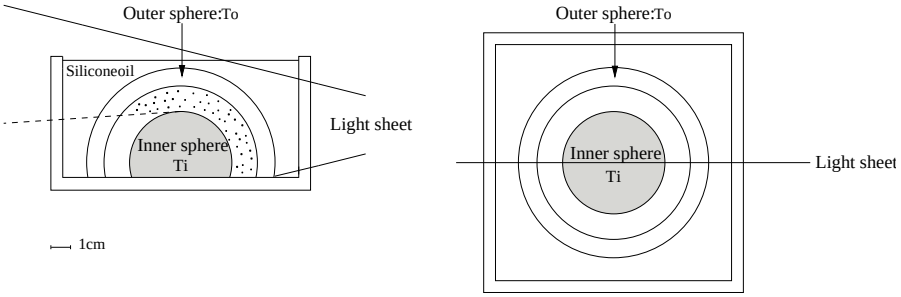

Fig. 9.3. The light sheet position.

that is to say between 2 and 3 pixels which give the lowest measurement uncertainty. For the particles utilized in this experiment, the gravitational velocity is found to be: $v_g = 2.9 \cdot 10^{-7}$m/s with M20 oil and $v_g = 3 \cdot 10^{-6}$m/s with M3 oil, which are disturbances that can be disregarded. The investigations were carried out in a meridional light sheet (figure 9.3) through the sphere's center.

For small ΔT between the two spheres we have the laminar convective state, and the flow structures of the PIV measurement (see figure 9.4) are in good agreement with the streamlines computed numerically by Garg [302]. We have an upward flow of 0.1 cm/s at the inner sphere and a downward flow of 0.05 cm/s at the outer sphere, and a ratio of 2 to 1 which has also been predicted theoretically by Mack & Hardee [303], and at the north pole we have a radial outward flow of 0.2 cm/s whereas in the equatorial region we have an area of zero velocity in the middle of the sphere as in the model of Garg [302].

By increasing the ΔT a time dependent pulsating ring vortex sets in at the north pole near the outer sphere (see figure 9.4). The maximal velocities increase up to 1 cm/s in the polar region and we have an upward flow of about 0.35 cm/s at the inner sphere and a downward flow of 0.1 cm/s at the outer sphere. The convective motion is dominant at the boundary regions and near to the pole in contrast to the vanishing velocities in a wide range of radial positions. Additionally there are small radial inward flows at the outer sphere boundary which is in agreement with the numerical simulations.

The Couette flow study required the use of another setup: the velocity being contained between 5 cm/s and 10 cm/s and therefore the previous delay used between each frame was too large. As a consequence, a pulsed Nd:YAG laser synchronized with a large format video camera was used allowing us to select appropriate pulse delays. The frame-straddling technique was employed for directional ambiguity removal. The study has been performed at 0.4 cm above the pole region (figure 9.5). The rotation of the inner sphere was 250 revolutions per minute for the experiment and $\Delta T = 0$. The velocity vector maps are presented in figure 9.6. The PIV parameters used for this investigation are listed in table 9.3.

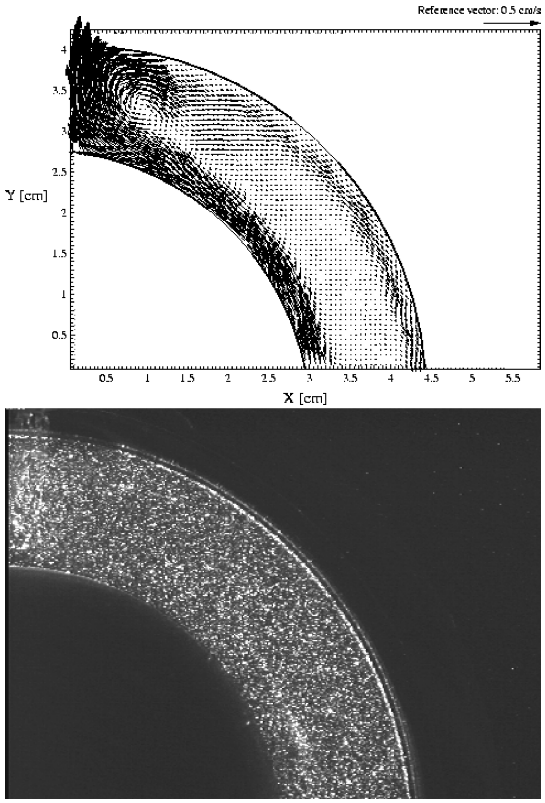

Fig. 9.4. Thermal convection velocity fields and flow picture with the two exposures.

Table 9.3. PIV recording parameters for Couette flow.

Flow geometry	$U_\infty = 10\,\mathrm{cm/s}$ parallel to light sheet
Maximum in-plane velocity	$U_{\max} \approx 10\,\mathrm{cm/s}$
Field of view	$50 \times 50\,\mathrm{mm}^2$
Interrogation volume	$1.6 \times 1.6 \times 2\,\mathrm{mm}^3$ ($H \times W \times D$)
Dynamic spatial range	DSR $\approx 31:1$
Dynamic velocity range	DVR $\approx 200:1$
Observation distance	$z_0 \approx 0.5\,\mathrm{m}$
Recording method	dual frame/single exposure
Ambiguity removal	frame separation (frame-straddling)
Recording medium	full frame interline transfer CCD (1008×1018 pixel)
Recording lens	$f = 60\,\mathrm{mm}$, $f_\# = 2.8$ to 22
Illumination	Nd:YAG laser[a], 70 mJ/pulse
Pulse delay	$\Delta t = 20\,\mathrm{ms}$
Seeding material	glass particles ($d_\mathrm{p} \approx 10\,\mu\mathrm{m}$)

[a] frequency doubled

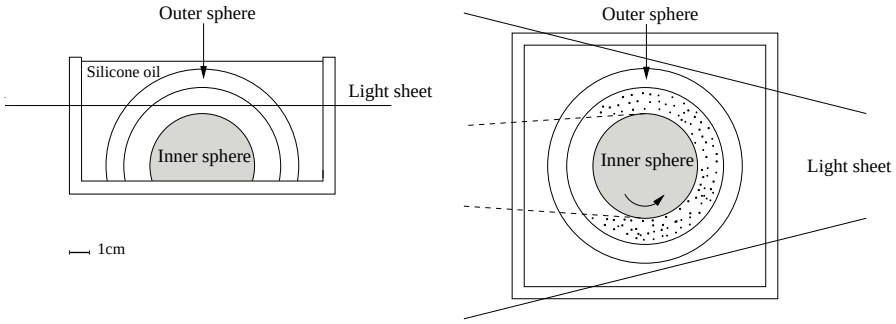

Fig. 9.5. The light sheet position: 0.4 cm up to the pole region.

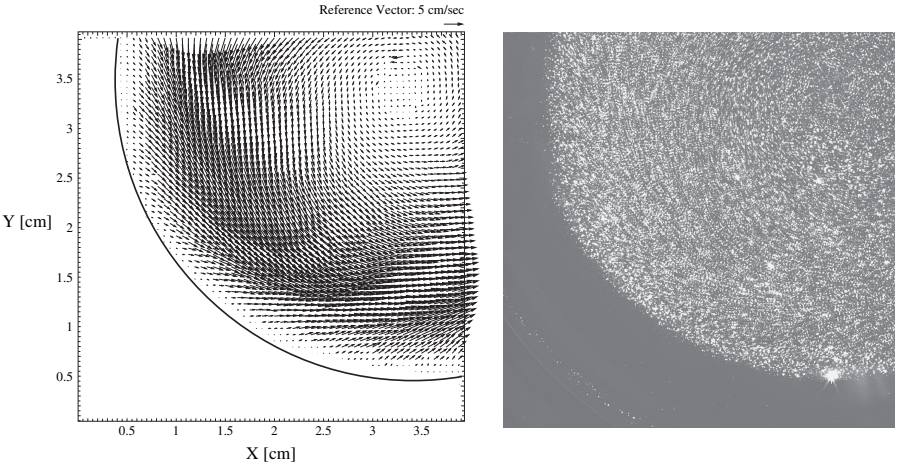

Fig. 9.6. Couette flow velocity field and picture with the two exposures.